Received 4 September 2023; revised 2 October 2023; accepted 4 October 2023. Date of publication 6 October 2023; date of current version 25 October 2023.

Digital Object Identifier 10.1109/OJCOMS.2023.3322592

Performance Analysis of Subband Full Duplex for 5G-Advanced and 6G Networks Through Simulations and Field Tests

XINGGUANG WEI[1,2], JIAN LI[1,2], CHUNLI LIANG[1,2], XIANGHUI HAN[1,2], MIN REN[1,2], AND RUIQI LIU[1,2] (Member, IEEE)

[1]Wireless Research Institute, ZTE Corporation, Shenzhen 518057, China

[2]State Key Laboratory of Mobile Network and Mobile Multimedia Technology, Shenzhen 518055, China

CORRESPONDING AUTHOR: J. LI (e-mail: li.jian17@zte.com.cn)

ABSTRACT As an essential technology in the evolution towards full duplex, the subband full duplex (SBFD) operation has attracted significant attention from both the academic and industrial communities, as well as global standardization bodies for its capability to increase the user perceived throughput (UPT) and the uplink coverage, reduce the transmission latency and support various traffics with different requirements in the same cell in time division duplexing (TDD) bands. In this paper, the model of a SBFD based communication system is clearly presented, along with the interference. To facilitate the early deployment of SBFD in 5G-Advanced and 6G networks, comprehensive performance evaluations on UPT, latency and coverage under different scenarios, different SBFD patterns and different traffics are conducted to explore the potential of the SBFD operation. Furthermore, a field test is carried out to verify the practical performance of SBFD in a typical outdoor scenario. Results obtained from both the simulations and field tests demonstrate significant performance gain for SBFD compared with traditional division duplexing schemes, especially for uplink transmissions.

INDEX TERMS Subband full duplex (SBFD), 6G, user perceived throughput (UPT), latency, field test, trial.

I. INTRODUCTION

EVER since the first generation of mobile communication system, half duplex operation for downlink (DL) and uplink (UL) has been applied to both the base station (BS) and the user equipment (UE), through time division duplexing (TDD) and frequency division duplexing (FDD) [1]. In this context, some research efforts were devoted to optimize the performance of the communication system by developing more flexible resource allocation [2], [3], [4]. However, with the booming development of the mobile communication industry towards the 6th generation (6G) [5], half duplex operation has become a major limiting factor for the overall system spectrum efficiency for the cellular networks [6], [7]. In addition, since future networks are expected to support both private users as well as vertical industries [8], half duplex suffers from its inflexibility in supporting various traffic types in a same cell. To improve the overall system spectrum efficiency and adaptability for different applications in the mobile communication system, full duplex operation has gained interests from both academic and industrial research communities [9], [10], [11].

The ultimate goal of full duplex operation is to support in-band full duplex (IBFD), where DL subband for DL transmission and UL subband for UL transmission are partially or fully overlapped [12]. Theoretically, compared with half duplex, IBFD can harvest doubled spectrum efficiency if the interference is perfectly suppressed. However, considering the technical challenges and costs of implementing IBFD, subband full duplex (SBFD) emerges as a more feasible solution [7], [13], [14]. SBFD is a preliminary version of full duplex, where DL subband for DL transmission and UL subband for UL transmission are not overlapped. Thus,

the implementation complexity and interference mitigation requirements in SBFD system are relaxed compared to IBFD systems [10]. To drive the innovation towards full duplex, the 3rd generation partnership project (3GPP) has approved a Release 18 study item to study the evolution of duplex operation for 5th generation-advanced (5G-A) and potentially 6G focusing on SBFD in TDD band [15]. The motivation of this study item is mainly to address the issues of TDD system identified in the field, including latency, coverage and flexibility on supporting various traffic types with different requirements in the same cell.

The concept of SBFD is first in 2021 under the name of XDD [16], where the authors present self-interference suppression techniques (i.e., a combination of antenna isolation and digital self-interference cancellation) and demonstrate 2.37 times UL coverage enhancement for SBFD compared to TDD. A proof-of-concept (PoC) with one transmit antenna and one receive antenna developed by the authors is tested in an anechoic chamber to demonstrate the feasibility of the proposed SBFD scheme. The authors of [10] propose interference mitigation schemes for SBFD operations, providing both simulation results and test results obtained by their PoC. Multiple interference suppression schemes are designed and evaluated in both dense urban and indoor scenarios. However, the SBFD performance evaluations focus only on a single SBFD pattern (i.e., SBFD pattern 1 as described in Section III of this paper) and a single traffic type. Recently, authors in [14] present precise modeling of different interference types and provide simulation results with rich details. Metrics including average DL and UL user throughput and 5th percentile user throughput are evaluated under different ratio of self-interference (RSI) values to show the performance improvement of the proposed SBFD scheme over traditional TDD schemes. However, the network performance should be considered globally by taking into account more metrics, such as the latency. The existing literature on SBFD mainly focus on interference mitigation techniques, while the performance evaluations are conducted only under some scenarios with a limited number of configurations, which might not be able to reflect the true performance of SBFD in practical deployment scenarios. Comprehensive performance analysis and comparison for SBFD considering the different subband patterns, traffic types and deployment scenarios on top of the existing 5G-A specifications are still missing. To the best of the authors' knowledge, there exists no literature providing comprehensive evaluations of the SBFD operation by considering both throughput and latency, and also verify the performance by a PoC in practical 5G networks. Considering that SBFD is likely to be specified in 3GPP Rel-19 5G-A specification and be commercialized after the standardization, the performance analysis of SBFD under different scenarios and different configurations are essential and this paper intends to fill in this gap. The main contributions of this work are listed as follows.

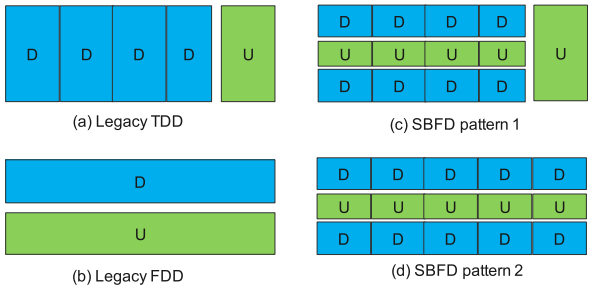

FIGURE 1. Different duplex modes.

- We present detailed and comprehensive SBFD performance evaluations for different scenarios, different SBFD patterns, different traffic types and different UE locations, including performance analysis for user perceived throughput (UPT), latency and coverage.
- We develop a SBFD PoC which is fully compatible with 5G networks, and conduct field trials practical in outdoor scenarios instead of laboratory to demonstrate the performance of it. Both peak data rate and end-to-end (E2E) latency are measured.
- We summarize the performance evaluation and analysis based on the simulation results and field tests, and provide some deployment recommendations for SBFD systems to facilitate the early deployment of SBFD.

The remaining of this paper is organized as follows. Section II introduces the system model including SBFD framework, scenario and detailed interference model. Section III presents the simulation assumptions as well as results for UPT, latency and coverage in both DL and UL. In Section IV, results obtained from field tests are introduced to verify the feasibility and demonstrate the performance of SBFD operations in practical environment. Section V highlights deployment recommendations for SBFD based on simulations and field test results. Finally, Section VI concludes this paper.

II. SYSTEM MODEL

A. SBFD FRAMEWORK

As explained in Fig. 1, the TDD and FDD systems partition resources for DL and UL in time domain and frequency domain, respectively. However, the SBFD system partitions resources for DL and UL in both time domain and UL domain, which provides flexibility for adaptation to different traffic types. Based on the latest 5G specification, almost all the bands above 3 GHz are designated as TDD band for new radio (NR) [17]. Compared with TDD, SBFD increases UL transmission opportunities for UL, which further increases UL coverage and UL throughput performance. On top of TDD duplex mode, dynamic TDD is introduced to dynamically update the DL and UL resource partition in time domain, which makes it impossible to avoid co-channel interference between base stations and between UEs [7], [14]. Compared with dynamic TDD, SBFD system

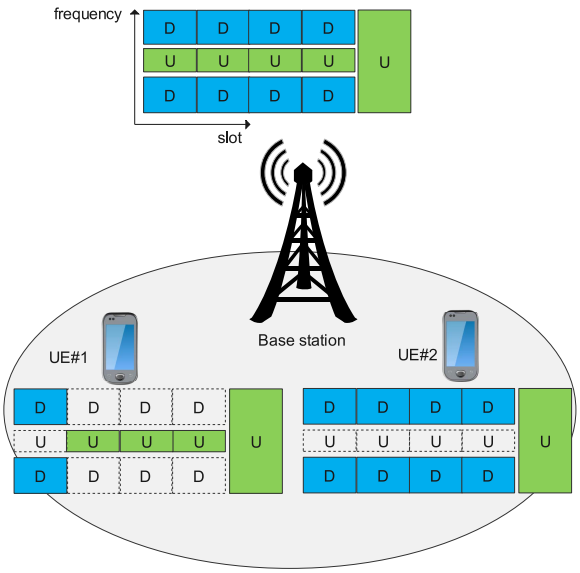

FIGURE 2. SBFD base station with half duplex UEs.

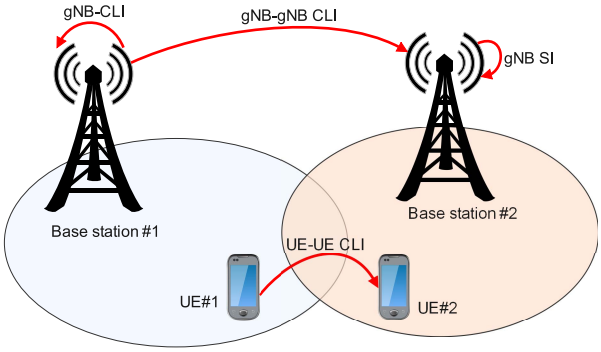

FIGURE 3. The general interference model of SBFD.

can avoid the serve co-channel interference between base stations and between UEs.

For SBFD, the DL subband for DL transmission and UL subband for UL transmission are not overlapped. In frequency domain, typical frequency resource partition between DL and UL for SBFD is "DUD" and "DU". For "DUD" pattern, the uplink resources for UL subband are allocated in between of DL subbands, which provide more frequency isolation for the UL subband in terms of adjacent gNB-to-gNB cross link interference (CLI). However, "DU" pattern simplifies the specification and implementation design since the downlink resources are contiguous within the bandwidth. In time domain, as shown in Fig. 1, it is possible to configure all the symbols or partial symbols in each TDD period as SBFD symbol that supports simultaneous DL and UL transmission. If all the symbols are configured as SBFD symbol (denoted as SBFD pattern 2), the DL transmission chances and UL transmission chances can be maximized. However, it also incurs CLI in all the symbols. On the other hand, if only partial symbols are configured as SBFD and other symbols are kept as DL symbol or UL symbol (denoted as SBFD pattern 1), the DL symbol and UL symbols can be applied to protect the important or sensitive transmissions.

For 6G, it is expected for both BS and UE to support SBFD operation to some extent, i.e., both BS and UE support simultaneous DL transmission in the DL subband and UL transmission in the UL subband [18]. However, in the phase of 5G-A, considering the legacy UEs in the field and implementation complexity and cost for supporting SBFD at UE side, SBFD base station with half duplex UE is the most feasible evolution path. In our simulation, SBFD base station with half duplex UE is assumed [7].

As shown in Fig. 2, the SBFD base station configured with "DUD" pattern is serving two half duplex UEs, i.e., UE#1 and UE#2. UE#1 performs DL in the first 1 slot and performs UL in the last 4 slots. On the contrary, UE#2 performs DL in the first 4 slots and performs UL in the last slot.

B. SCENARIO

As a promising technology for 5G-A and 6G, SBFD stands out for its advantages of increasing UPT targeting enhanced mobile broadband (eMBB) traffic, reducing the transmission latency for ultra-reliable low latency communication (URLLC) traffic, increasing the UL coverage and satisfying different communication requirements in the same cell thanks to the simultaneous DL&UL transmission and flexible subband configuration. It is pivotal to investigate the potential of SBFD in different scenarios before the practical deployment.

Firstly, increasing UPT is urgent for dense urban macro scenario and indoor hotspot scenario since uplink-heavy eMBB traffic typically occurs in dense urban macro scenario and indoor hotspot scenario, e.g., video surveillance and machine vision. Secondly, latency reduction is essential for indoor hotspot scenario (e.g., smart factory) since uplink URLLC traffic typically occurs in indoor hotspot scenario, e.g., factory panoramic monitoring and remote control. Thirdly, coverage enhancement is attractive for almost all the outdoor scenarios, e.g., urban macro scenario and dense urban macro scenario. Considering all these aspects, dense urban macro scenario and indoor hotspot scenario are selected as the simulation scenarios. Indoor hotspot scenario represents the scenario with lower transmission power and smaller inter-site distance (ISD), while dense urban macro scenario represents the scenario with higher transmission power and larger ISD.

C. INTERFERENCE MODEL

In order to reflect the practical challenges and performance gain, the interference in SBFD has to be clearly modelled. Compared with the legacy TDD scenario, as depicted in Fig. 3, the following new types of interference are considered in our system. Overall, the interference models employed in this study follow the 3GPP technical report [15]. In this paper, SI, gNB-CLI and gNB-gNB CLI are all referred as gNB-side interference.

TABLE 1. Notation summary.

Notation	Description
N_{DLRB}	Total number of resource blocks (RBs) in DL subbands
N_{ULRB}	Total number of RBs in UL subbands
P_{tx}^{max}	Maximum gNB DL Tx power in the two DL subbands
P_{tx}	The gNB DL Tx Power on the two DL subbands

- gNB[1] self-interference (SI): The interference generated by the DL transmission in the DL subband to the UL reception in the UL subband in the same cell.
- gNB co-site inter-sector inter-subband CLI (gNB-CLI): The interference generated by the DL transmission in the DL subband in one sector to the UL reception in the UL subband in another sector of the same base station.
- gNB-gNB inter-site inter-subband CLI (gNB-gNB CLI): The interference generated by the DL transmission in the DL subband in one base station to the UL reception in the UL subband in another base station.
- UE-UE inter-subband CLI (UE-UE CLI): The interference generated by the UL transmission in the UL subband in one UE to the DL reception in the DL subband in another UE.

In this section, we introduce the detailed interference models applied in our simulation. The summary of notations used in this paper can be found in Table 1.

1) GNB SI

Typically, the SI is frequency flat within the UL subband, especially if guard band is applied in between the DL suband and UL subband [19]. Thus, a subband level SI suppression capability can be defined. Different SI suppression capabilities are required in case of different DL transmission power. To consider the worst case, the subband level SI suppression capability α_{SI} is defined as the overall SI suppression capability for UL subband when all the DL RBs in the DL subbands are allocated with maximum gNB DL Tx power.

The value of α_{SI} is calculated according to the UL receiver sensitivity degradation, noise floor of UL subband and maximum gNB DL Tx Power as below:

$$\alpha_{SI} = \frac{P_{tx}^{max}}{I_{SI}^{max} \times \left(\frac{N_{DLRB}}{N_{ULRB}}\right)} \tag{1}$$

I_{SI}^{max} is the residual self-interference power on the UL subband when all the DL RBs in the DL subbands are allocated with maximum gNB DL Tx power. I_{SI}^{max} is determined by the receiver sensitivity degradation. SBFD base station receiver sensitivity degradation of 1 dB has been endorsed as tentative requirement for SBFD gNB in 3GPP RAN4 study [15]. In this case, I_{SI}^{max} can be derived by $10 \times log_{10}(\frac{I_{SI}^{max}+N}{N}) = 1$ dB, where N is the noise floor over the UL subband given by $N = -174$ dBm $+ 10 \times log_{10}(20 \times 10^6) + 5 = -96$ dBm, assuming 20MHz UL subband and 5 dB noise figure.

1. gNB stands for "next generation NodeB", which is the name of 5G BSs in 3GPP standard series.

In the simulation, according to the above analysis and simulation assumptions introduced in the next section, α_{SI} for indoor hotspot scenario and dense urban macro scenario is calculated as below.

- For indoor hotspot with $P_{tx}^{max} = 24$ dBm, $\alpha_{SI} = 118.9$ dB.
- For dense urban macro with $P_{tx}^{max} = 44$ dBm, $\alpha_{SI} = 138.9$ dB.

Once the SI suppression capability for each scenario is determined, the SI in our simulation can be modeled as

$$I_{SI} = \frac{P_{tx}}{\alpha_{SI} \times \left(\frac{N_{DLRB}}{N_{ULRB}}\right)}. \tag{2}$$

2) GNB-CLI

gNB-CLI is similar as gNB SI. The main difference is that, gNB-CLI is from different sectors in the same base station while the gNB SI is from the same sector in the base station. Nevertheless, the interference models for gNB-CLI and SI are similar. To consider the worst case, a subband level gNB-CLI suppression capability is defined as the overall gNB-CLI suppression capability for UL subband when all the DL RBs in the DL subbands in another sector are allocated with maximum gNB DL Tx power. Then, the gNB-CLI in the UL subband on a single receiver chain is modelled as

$$I_{co-site} = \sum_{sectors} \frac{P_{tx}^{sectors}}{\alpha_{co-site} \times \left(\frac{N_{DLRB}}{N_{ULRB}}\right)}, \tag{3}$$

where $P_{tx}^{sectors}$ is the DL transmission power of sectors during the simulation. The BS has to provide at least the same interference suppression capability as the SI suppression capability for gNB-CLI. In our simulation, the same value of α_{SI} is applied to $\alpha_{co-site}$ across different scenarios.

3) GNB-GNB CLI

The gNB-gNB CLI experienced by the victim gNB on each receiver chain for the UL subband can be modelled as

$$\begin{aligned} I_{gNB-gNB-CLI} &= \sum_{n} I_{inter-cite-CLI}^{per-RB}(n) \\ &= P_{tx}^{max} \times \frac{N_{used-RB-DL}}{N_{DLRB}} \times CL^{BS} \\ &\quad \times \left(\frac{1}{ACLR_{BS}} + \frac{1}{ACS_{BS}}\right) \times \frac{N_{DLRB}}{N_{ULRB}}, \end{aligned} \tag{4}$$

where $I_{inter-cit-CLI}^{(per-RB)}(n)$ represents the power of inter-site gNB-gNB inter-subband CLI from aggressor gNB to victim gNB on each receiver chain at UL RB n, $N_{used-RB-DL}$ is the number of DL RBs allocated for DL transmission by aggressor gNB, CL^{BS} is the coupling loss between aggressor gNB and victim gNB, accounting for beamforming at the aggressor gNB and victim gNB. $ACLR_{BS}$ and ACS_{BS} are gNB adjacent channel leakage ratio (ACLR) and gNB adjacent-channel selectivity (ACS), respectively. In the simulations, $ACLR_{BS} = 45$ dB and $ACS_{BS} = 46$ dB, which are typical values specified for 5G base station by 3GPP standards [17].

4) UE-UE CLI

The interference power of UE-UE inter-subband CLI experienced by the victim UE on each receiver chain can be modelled as

$$I_{UE-UE-CLI} = \sum_{m} I^{per-UE}_{UE-UE-CLI}(m) = \sum_{m} I_{UE-UE,IBE}(m) \times CL + P^{UE}_{tx} \times CL \times \frac{1}{ACS_{UE}} \times \frac{N_{DLRB}}{N_{ULRB}}, \quad (5)$$

where $I^{perUE}_{UE-UE-CLI}(m)$ is the power of UE-UE inter-subband CLI from aggressor UE to victim UE on each receiver chain at one DL RB m based on the in-band emission model, P^{UE}_{tx} is UL transmission power of aggressor UE across all transmit chains over the allocated UL RBs and CL is the coupling loss between aggressor UE and victim UE, accounting for analog beamforming at the aggressor UE and victim UE. ACS_{UE} is the UE ACS, which is set to 33 dB in the simulations according to 3GPP standards [17]. $I_{UE-UE,IBE}(m)$ is the in-band emission, which can be modelled following the definition given in section 6.4.2.3 of technical specification (TS) 38.101–1 [17].

III. PERFORMANCE EVALUATION OF SBFD

Although some advanced TDD schemes are introduced for 5G, such as dynamic TDD [14], the semi-static TDD is the only widely deployed TDD system around the world. Thus, semi-static TDD system is chosen as the baseline scheme for comparison with SBFD in the simulations. To compare the system performance of SBFD with baseline TDD, DL/UL UPT, DL/UL latency and coverage are evaluated. The UPT and latency are evaluated via system level simulation (SLS) under different SBFD patterns, different scenarios and different traffic types. The coverage is evaluated via link level simulation (LLS) plus link budget analysis.

A. SLS SIMULATION ASSUMPTION

In this section, we introduce the evaluation assumptions of UPT and latency, which are summarized in Table 2. Specifically, as per 3GPP standards, there are 14 orthogonal frequency-division multiplexing (OFDM) symbols per slot and there is a gap of 1 symbol between X and U symbols.

Overall, the simulator follows the 5G NR evaluation methodology as specified in a corresponding 3GPP report [20]. When conducting such simulations, good practices are applied to ensure trustworthy results. UEs are dropped independently with uniform distribution for indoor hotspot scenario and are dropped in cluster distribution for dense urban macro scenario over predefined area of the network layout. After dropping UEs, the locations of UEs and gNB remain unchanged.

SBFD patterns: In our study, the baseline is legacy TDD configured as "DDDSU" and configured with 100 MHz (273 RBs), where the ratios of UL resource and DL resource are about 20% and 77.14%, respectively. In order to provide comprehensive results for SBFD, as listed below and depicted in Fig. 1, two SBFD patters with "DUD" frequency resource partition are analyzed in our simulation. For both SBFD patterns, the DL subband is configured as 104 RBs in each side of the "DUD" pattern and the UL subband is configured as 55 RBs. There are also 5 RBs as guard band in between the DL subband and UL subband to provide frequency isolation between DL subband and UL subband.

TABLE 2. SLS assumptions for SBFD evaluation.

Scenario	Indoor office	Dense urban (macro layer)
Layout	120 m × 50 m indoor office, 12 BSs in a single layer.	Hexagon grid macro layer, cell 7 macro cites, 3 sectors per site.
ISD	20 m	200 m
Frequency	4 GHz	
Bandwidth	100 MHz	
Numerology	30 kHz sub-carrier spacing (SCS)	
BS TX power	24 dBm per 100 MHz	44 dBm per 100 MHz
UE TX power	23 dBm	
Frame structure	Legacy TDD: DDDSU, S=[12D:2G:0U] SBFD Pattern 1: XXXXU, SBFD Pattern 2: XXXXX X = 'D:U:D', pattern = 104:55:104.	
BS antenna radiation pattern	Wall-mount model in Table A.2.1-7 in TR 38.802 [20].	3-sector BS radiation model in Table A.2.1-7 in TR 38.802 [20].
BS antenna configuration	**Legacy TDD**: (M,N,P,Mg,Ng;Mp,Np)= (4,4,2,1,1;4,4) (d_H, d_V) = (0.5,0.5)λ +45°/-45° polarization. **SFBD**: two panel groups, each panel group with (M,N,P,Mg,Ng;Mp,Np) =(4,4,2,1,1;4,4) (d_H, d_V) = (0.5,0.5)λ +45°/-45° polarization. $(d_{a,H}, d_{a,V})$ = (0, 4)λ	**Legacy TDD**: (M,N,P,Mg,Ng;Mp,Np)= (8,8,2,1,1;2,4) (d_H, d_V) = (0.5,0.8)λ +45°/-45° polarization. **SFBD**: two panel groups, each panel group with (M,N,P,Mg,Ng;Mp,Np) =(8,8,2,1,1;2,8) (d_H, d_V) = (0.5,0.8)λ +45°/-45° polarization. $(d_{a,H}, d_{a,V})$ = (0, 4)λ
Receiver noise figure	5 dB for BS, 9 dB for UE	
UE receiver type	MMSE-IRC, UE processing capability 1	
UE antenna configuration	2 Tx and 4 Rx antenna ports. 2Tx: (M,N,P,Mg,Ng;Mp,Np)=(1,1,2,1,1;1,1) (d_H, d_V) = (N/A, N/A)λ, 0°/90° polarization 4Rx: (M,N,P,Mg,Ng;Mp,Np)=(1,2,2,1,1;1,2) (d_H, d_V) = (0.5, N/A)λ, 0°/90° polarization	
UE power control	$P_0 = -60$ dBm, $\alpha = 0.6$	$P_0 = -86$ dBm, $\alpha = 0.8$
UE density	10 UEs per BS	20 UEs per BS

- SBFD pattern 1: the "DUD" pattern is applied in the first 4 slots in each TDD period. Pure "U" slot is configured in the last slot in each TDD period. During this "U" slot, there is no CLI. Thus, the important or sensitive uplink signal can be protected in this slot. Ratios of UL resource and DL resource in each TDD period are about 35.83% and 59.86%, respectively. Compared with baseline TDD, the UL resource is increased by about 79.15%, while the DL resource is reduced by 22.40%.
- SBFD pattern 2: the "DUD" pattern is applied in all the 5 slots in each TDD period, where both DL and UL have 5 transmission chances in each TDD period. In this case, ratios of UL resource and DL resource in each TDD period are about 20.15% and 76.19%, respectively, which are almost the same as those for legacy TDD.

Traffic model: Three key usage scenarios were defined by The international telecommunication union (ITU) for IMT-2020, namely, eMBB, URLLC and massive machine type communication (mMTC). Recently, ITU defined usage scenarios and overarching aspects of IMT-2030, in which evolved eMBB and URLLC still play prominent roles [21]. In order to investigate the potential of SBFD for 5G-A and 6G networks, both eMBB traffic and URLLC traffic are evaluated in our system. The eMBB traffic and URLLC traffic are generated by FTP traffic model 3 (FTP3) with different packet sizes [14].

- eMBB traffic: 0.5M bytes and 0.125M bytes packet size for DL and UL, respectively. eMBB traffic tends to cause CLI to other base stations and UEs since it requires more slots to transmit the packet with larger packet size. Typical traffic corresponding to larger packet size is extended reality (XR).
- URLLC traffic: 4K bytes and 1K bytes packet size for DL and UL, respectively. URLLC traffic causes less CLI to other base stations and UEs since it requires less slots to transmit the packet with smaller packet size. Typical traffic corresponding to smaller packet size is remote control in the smart industry.

Antenna pattern: One of the most critical issues in SBFD system is to suppress the self-interference. In order to provide sufficient self-interference suppression capability for SBFD base station, the Tx antenna panel and Rx antenna panel need to be separated to provide antenna isolation [14]. In our simulation, the total number of antenna elements of the antenna array for SBFD is assumed as two times of the total number of antenna elements of the antenna array for baseline TDD. The total number of transmission and reception radio frequency units (TxRUs) of the antenna array for SBFD is the assumed the same as the total number of TxRUs of the antenna array for legacy TDD. Although this requires to double the number of elements and double the size of the antenna panel, it helps to avoid compromising the available performance of SBFD.

Performance metrics: To demonstrate the potential gain of SBFD, two performance metrics are applied in our SLS, i.e., UPT and packet latency.

UPT is defined as the size of an FTP packet divided by the time duration which starts when the packet is received in the transmit buffer and ends when the last bit of the packet is correctly delivered to the receiver. Mean, 5th percentile, 50th percentile and 95th percentile UPT is applied in our simulation. For simplicity, the mean, 5th percentile, 50th percentile and 95th percentile UPT for DL is referred as DL-mean, DL-5%, DL-50% and DL-95% UPT, respectively. Similarly, the mean, 5th percentile, 50th percentile and 95th percentile UPT for UL is referred as UL-mean, UL-5%, UL-50% and UL-95% UPT, respectively.

The mean UPT is mean value of average UPTs for all users, which is an indicator to reflect the overall system performance. In addition, the DL-5% UPT and UL-5% UPT reflect the DL UPT and UL UPT for cell-edge UEs, respectively, since the cell-edge UEs generally experience lower UPT. The DL-95% UPT and UL-95% UPT reflect the DL UPT and UL UPT for cell-center UEs, respectively, since the cell-center UEs generally experience higher UPT. Therefore, the DL UPT and UL UPT for cell-edge UEs refer to DL-5% UPT and UL-5% UPT in this paper, respectively. The DL UPT and UL UPT for cell-center UEs refer to DL-95% UPT and UL-95% UPT in this paper, respectively.

Packet latency is defined as the time duration which starts when the packet is received in the transmit buffer and ends when the last bit of the packet is correctly delivered to the receiver. Latency reduction is more crucial for UEs with satisfying coverage, because cell-edge UEs with poor coverage care more about the coverage instead of the latency. Thus, in this paper, the 50th percentile packet latency from the CDF for all these packets from all the UEs is applied as the metric to evaluate the overall latency performance in SBFD system.

B. SIMULATION RESULTS FOR UPT AND LATENCY

The resource utilization (RU) is applied to reflect the traffic load, which is defined as number of RBs per cell used by traffic for the given link direction during observation time divided by total number of RBs per cell available for traffic for the given link direction over observation time. In our simulation, low RU, medium RU and high RU correspond to RU $\leq$ 10%, 20% $\leq$ RU $\leq$ 40% and RU $\geq$ 50%, respectively. Correspondingly, low RU, medium RU and high RU refers to low traffic load, medium traffic load and high traffic load, respectively.

As analyzed in Section II, compared with baseline TDD and SBFD pattern 2, the DL resource of SBFD pattern 1 is reduced by around 22% and the UL resource of SBFD pattern 1 is increased by around 79%. This needs to be considered when comparing the performance between baseline TDD and SBFD pattern 1 and comparing the performance between SBFD pattern 1 and SBFD pattern 2.

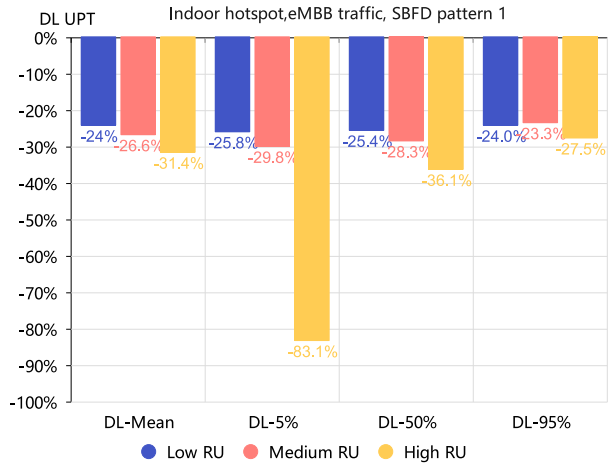

FIGURE 4. DL UPT for indoor hotspot with eMBB traffic and SBFD pattern 1.

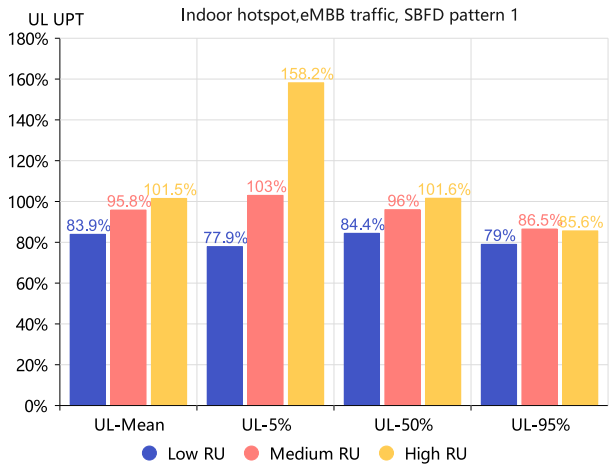

FIGURE 5. UL UPT for indoor hotspot with eMBB traffic and SBFD pattern 1.

1) SIMULATION RESULTS FOR EMBB TRAFFIC

For eMBB traffic, the results for indoor hotspot scenarios are presented from Fig. 4 to Fig. 8, and the results for dense urban scenarios are presented from Fig. 9 to Fig. 13, which will be elaborated further below.

As depicted in Fig. 4 and Fig. 5, simulation results are obtained on UPT for eMBB traffic with SBFD pattern 1 under indoor hotspot scenarios. Thanks to SBFD pattern 1, the DL mean UPT is decreased by 24% $\sim$ 31.4% due to the UE-UE CLI and reduced DL resources. The DL mean UPT loss is comparable with DL resources loss of SBFD pattern 1 in this case, which implies the overall impact of UE-UE CLI is small. For cell-edge UEs, DL UPT (i.e., DL-5% UPT) is decreased by 25.8% $\sim$ 29.7% in case of low and medium RU, which is comparable with the DL resource loss. However, for high RU, the DL UPT for cell-edge UEs is reduced by 83.1% due to the severer UE-UE CLI in case of high traffic load. For cell-centre UEs, the DL UPT (i.e., DL-95% UPT) is decreased by 23.9% $\sim$ 25.7%, which indicates the impact of UE-UE CLI is minor for cell-centre UEs since the DL UPT loss is almost identical to DL resource loss.

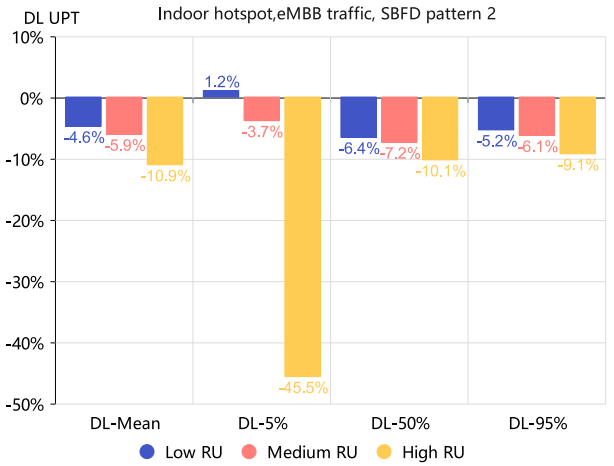

FIGURE 6. DL UPT for indoor hotspot with eMBB traffic and SBFD pattern 2.

The UL mean UPT is increased by 83.9% $\sim$ 95.8% in case of low and medium RU, which is much higher than the UL resource increase of SBFD pattern 1. However, in case of high RU, although there is still significant gain for mean UL UPT, i.e., 48.3%, it is smaller than the UL resource increase due to the larger gNB-side interference in case of high traffic load. For cell-centre UEs, the UL UPT (i.e., UL-95% UPT) is increased by 79% $\sim$ 86.5%. The gain for UL-95% UPT is basically agnostic to the traffic load, which implies that gNB-side interference has minor impact on cell-centre UEs thanks to the high signal to interference plus noise ratio (SINR) for cell-centre UEs even in case of UE-UE CLI.For cell-edge UEs, the UL UPT (i.e., UL-5% UPT) is increased by 77.9% $\sim$ 103%. It is worth noting that the gain of UL-5% UPT for medium RU is higher than that for low RU and high RU. The reason is, baseline TDD offers satisfactory UPT in case of low RU and it is difficult to demonstrate the gain for SBFD for this case. On the other hand, for the case of medium to high RU, the gain for SBFD is increased evidently due to the limited UL resource in legacy TDD systems. However, in case of high RU, the UPT for SBFD is also impacted by the gNB-side interference.

According to Fig. 6 and Fig. 7, numerical results on UPT for eMBB traffic with SBFD pattern 2 under indoor hotspot scenario can be given. The results are analyzed in both DL and UL. The DL mean UPT is decreased by 4.6% $\sim$ 10.9% due to the UE-UE CLI, where the loss of DL mean UPT increases with the traffic load since the UE-UE CLI increases with the traffic load. For cell-edge UEs, DL UPT (i.e., DL-5% UPT) is almost the same as that for baseline TDD in low and medium traffic load. However, in case of high traffic load, the DL UPT for cell-edge UEs is reduced by 45.5% due to the UE-UE CLI. For cell-centre UEs, the DL UPT (i.e., DL-95% UPT) is decreased by 5.2% $\sim$ 9.1% due to the UE-UE CLI. Overall, the UE-UE CLI has limited impact on the DL UPT for cell-centre UEs since the cell-centre UEs with good SINR can combat the UE-UE CLI. The mean UL UPT is increased by 9.2% $\sim$ 14.9%. For cell-edge UEs,

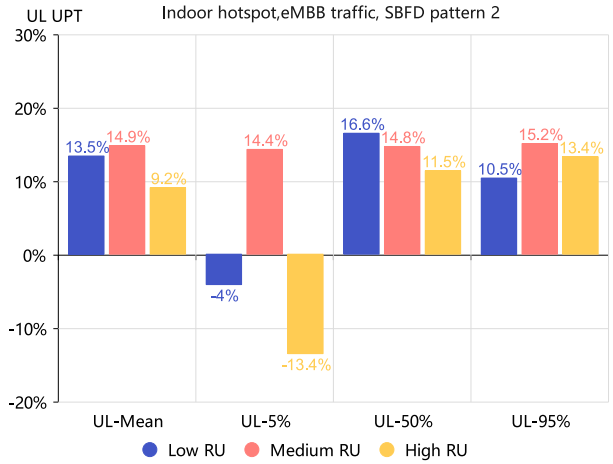

FIGURE 7. UL UPT for indoor hotspot with eMBB traffic and SBFD pattern 2.

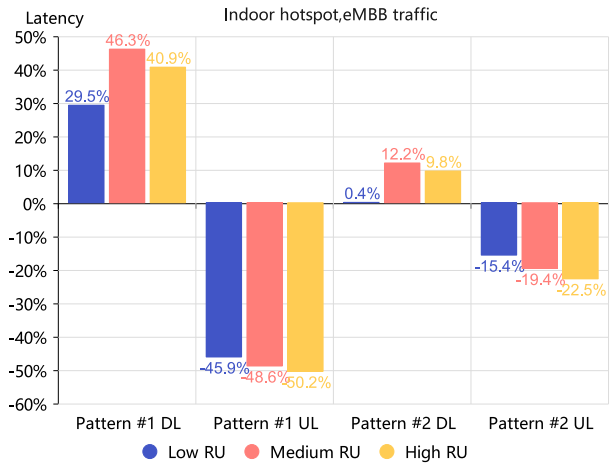

FIGURE 8. 50th percentile latency for indoor hotspot with eMBB traffic.

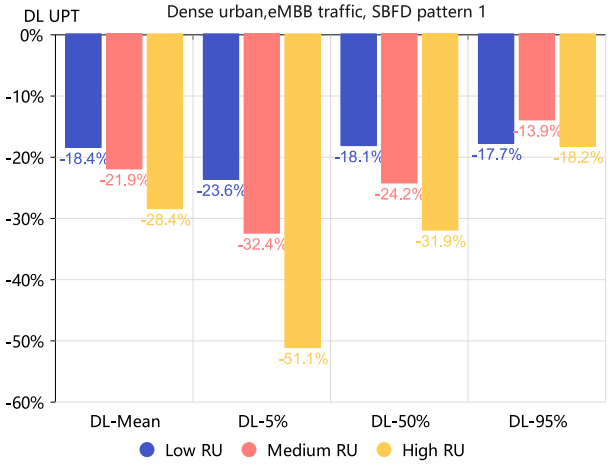

FIGURE 9. DL UPT for dense urban macro with eMBB traffic and SBFD pattern 1.

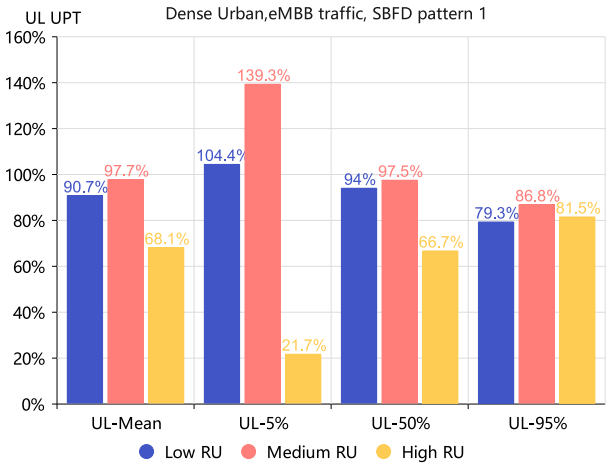

FIGURE 10. UL UPT for dense urban macro with eMBB traffic and SBFD pattern 1.

the UL UPT (i.e., UL-5% UPT) is slightly decreased at low traffic load. In case of the medium traffic load, the UL UPT is increased by 14.4% while in case of high traffic load, the UL UPT experiences a 13.4% loss due to the interference from gNB side. The reason is similar as above, the gain for medium traffic load is higher than low and high traffic load. For cell-centre UEs, the UL UPT (i.e., UL-95% UPT) is increased by 10.5% $\sim$ 15.2%. Similarly, the gNB-side interference has minor impact on cell-centre UEs since the UPT gain is similar under different traffic loads.

Fig. 8 depicts the packet latency for eMBB traffic in the indoor hotspot environment. For SBFD pattern 1, the DL 50th percentile latency is increased by 29.5%, 46.3% and 40.9% for low RU, medium RU and high RU, respectively. The UL 50th percentile latency is decreased by 45.9%, 48.6% and 14.2% for low RU, medium RU and high RU, respectively. Comparatively, for SBFD pattern 2, the DL 50th percentile latency is increased by 0.4%, 12.2% and 9.8% for low RU, medium RU and high RU, respectively. The UL 50th percentile latency is decreased by 15.4%, 19.4% and 22.5% for low RU, medium RU, and high RU, respectively.

Fig. 9 and Fig. 10 together present simulation results obtained on UPT for eMBB traffic with SBFD pattern 1 under dense urban scenarios. The DL mean UPT is decreased by 18.4% $\sim$ 28.4% due to the UE-UE CLI and reduced DL resources. Similarly, the DL mean UPT loss is comparable with DL resources loss, which implies the overall impact of UE-UE CLI is small. For cell-edge UEs, DL UPT (i.e., DL-5% UPT) is decreased by 23.6% $\sim$ 32.4% in case of low and medium RU, which is comparable with the DL resource loss. However, for high RU, the DL UPT for cell-edge UEs is decreased by 51.1% due to the increased UE-UE CLI in case of high traffic load. For cell-centre UEs, the DL UPT (i.e., DL-95% UPT) is decreased by 13.9% $\sim$ 18.2%, which is slightly smaller than DL resource loss. The reduced DL resources and UE-UE CLI have less impact on the cell-centre UEs thanks to the high SINR of cell-centre UEs. The UL mean UPT is increased by 90.7% $\sim$ 97.7% in case of low and medium traffic load, which is much higher than the UL resource increase. However, for high RU, although there is still gain for mean UL UPT, i.e., 28.5%, it is much smaller than the UL resource increase due to the gNB-side

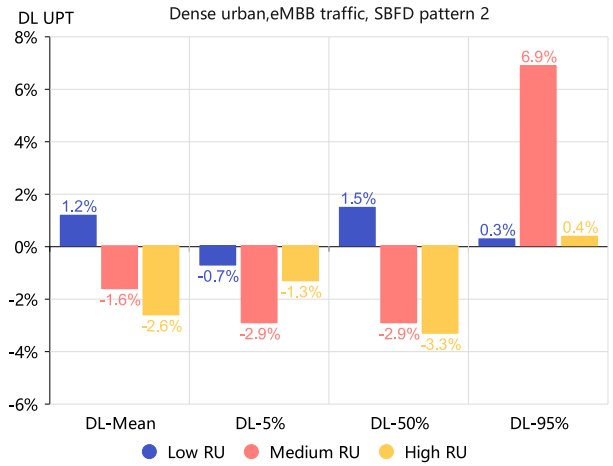

FIGURE 11. DL UPT for dense urban macro with eMBB traffic and SBFD pattern 2.

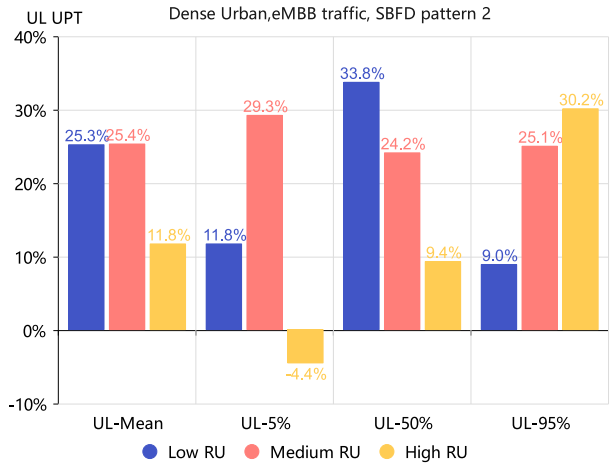

FIGURE 12. UL UPT for dense urban macro with eMBB traffic and SBFD pattern 2.

interference in case of high traffic load. For cell-edge UEs, the UL UPT (i.e., UL-5% UPT) is increased by 104.4% ∼ 139.3% in case of low and medium RU, which is much higher than the ratio of UL resource increment. However, in case of high RU, only 6.8% gain is observed for UL UPT for cell-edge UEs because cell-edge UEs are vulnerable to gNB-side interference especially in case of high traffic load. For cell-centre UEs, the UL UPT (i.e., UL-95% UPT) is increased by 78.8% ∼ 86.8%. The gain for cell-centre UEs is basically agnostic to the traffic load, which implies that gNB-side interference has minor impact on cell-centre UEs thanks to the high SINR for cell-centre UEs.

Fig. 11 and Fig. 12 depict the simulation results on UPT for eMBB traffic with SBFD pattern 2 under dense urban scenarios. In the DL, the mean UPT is almost the identical to that of baseline TDD. Furthermore, the DL UPT for cell-edge UEs and cell-centre UEs are also almost identical to that for baseline TDD, respectively. It indicates that the increased DL transmission chances can negate the impact of UE-UE CLI. In the UL, the mean UPT is increased by 11.8% ∼ 25.4%. For cell-edge UEs, the UL

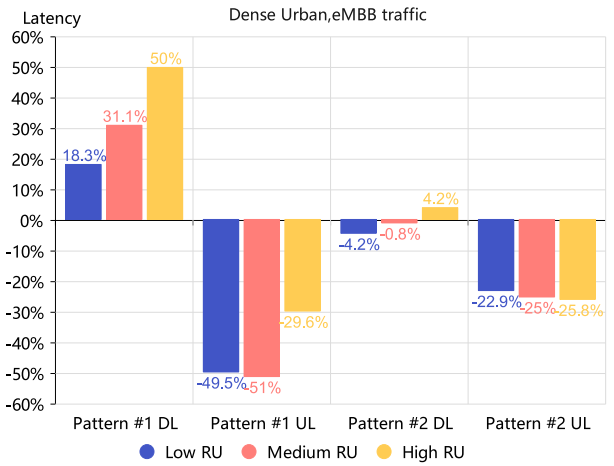

FIGURE 13. 50%-tile latency for dense urban macro with eMBB traffic.

UPT (i.e., UL-5% UPT) is increased by 11.8% ∼ 29.3% in case of low and medium traffic load. The UL UPT is decreased by 4.4% in case of high traffic load due to the gNB-side interference in case of high traffic load. For cell-centre UEs, the UL UPT (i.e., UL-95% UPT) is increased by 9.0% ∼ 30.2%. Unlike other cases, the UPT gain for cell-centre UEs is increasing with the traffic load. The reason is that, gNB-side interference has limited impact for UPT for cell-center UEs while the UL UPT for baseline TDD decreases with the increasing RU due to the limited UL transmission chance in each TDD period for baseline TDD.

As shown in Fig. 13, simulations on packet latency for eMBB traffic under dense urban scenarios are conducted. For SBFD pattern 1, the DL 50th percentile latency is increased by 18.3%, 31.1% and 50% for low RU, medium RU and high RU, respectively. The UL 50th percentile latency is decreased by 49.5%, 51% and 9% for low RU, medium RU and high RU, respectively. For SBFD pattern 2, the DL 50th percentile latency is almost the same as that for baseline TDD. The UL 50th percentile latency is decreased by 22.9%, 25.0% and 25.8% for low RU, medium RU and high RU, respectively.

2) SIMULATION RESULTS FOR URLLC TRAFFIC

Another traffic model we simulated for both indoor hotspot scenarios and dense urban macro scenarios is the URLLC traffic. The results for indoor hotspot are presented from Fig. 14 to Fig. 18, and the results for dense urban macro are presented from Fig. 19 to Fig. 23.

Fig. 14 and Fig. 15 together present the results on DL and UL UPT for URLLC in indoor hotspot scenarios with SBFD pattern 1. The DL mean UPT is basically identical to that for baseline TDD in case of low and medium RU, while the DL mean UPT is decreased by 10.3% due to the increased UE-UE CLI. For cell-edge UEs, the DL UPT (i.e., DL-5% UPT) is the same as that for baseline TDD in case of low and medium RU. However, the DL UPT is decreased by 52.2% due to UE-UE CLI in case of high RU.

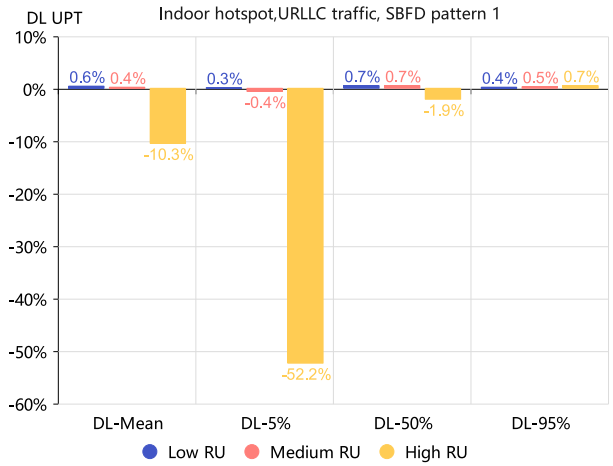

FIGURE 14. DL UPT for indoor hotspot with URLLC traffic and SBFD pattern 1.

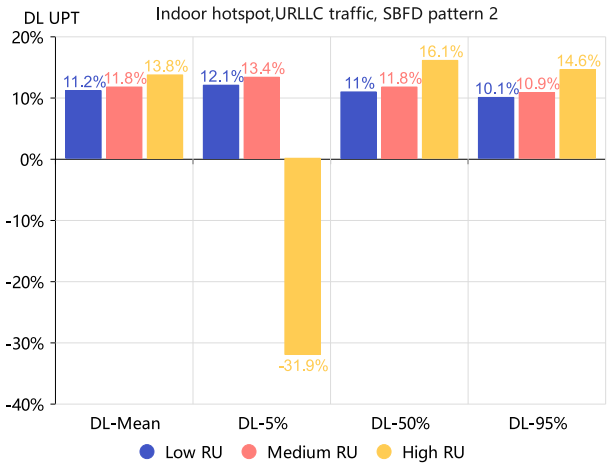

FIGURE 16. DL UPT for indoor hotspot with URLLC traffic and SBFD pattern 2.

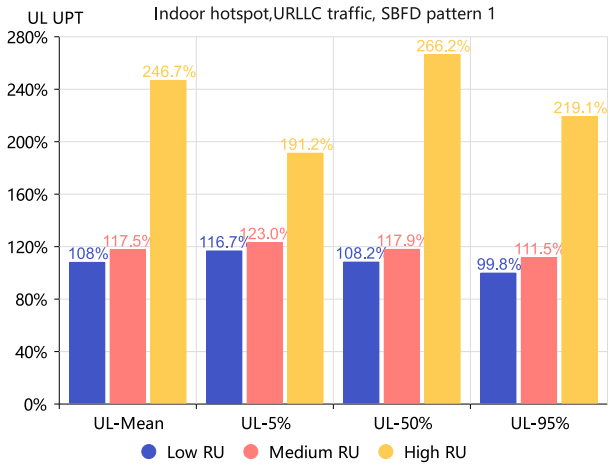

FIGURE 15. UL UPT for indoor hotspot with URLLC traffic and SBFD pattern 1.

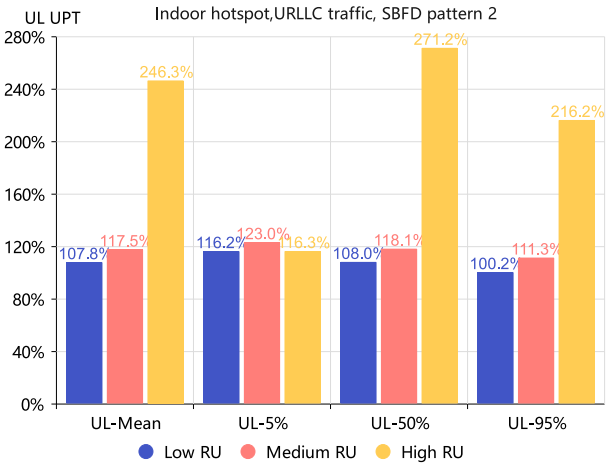

FIGURE 17. UL UPT for indoor hotspot with URLLC traffic and SBFD pattern 2.

For cell-centre UEs, the DL UPT (i.e., DL-95% UPT) is the same as that for baseline TDD. In the UL, the mean UPT is increased by 108%∼ 246.7%, which is much higher than the UL resource increase. The gain of UL UPT for cell-edge UEs and cell-centre UEs are similar, i.e., the UL UPT for cell-edge UEs and cell-centre UEs is increased by 116.7%∼ 191.2% and 99.8%∼ 219.1%, respectively. The UL UPT gain in case of high RU is much higher than that in case of low/medium RU since uplink is the bottom neck of baseline TDD in case of high traffic load, i.e., only one transmission opportunity is available for baseline TDD in each TDD period.

As depicted in Fig. 16 and Fig. 17, the following observations on UPT for URLLC traffic with SBFD pattern 2 under indoor hotspot scenarios can be given. In the simulations, the DL mean UPT is increased by 11.2% ∼ 13.8%. For cell-edge UEs, the DL UPT (i.e., DL-5% UPT) is increased by 12.1% ∼ 13.4% in case of low and medium RU. However, the DL UPT is decreased by 31.9% due to UE-UE CLI in case of high RU. For cell-centre UEs, the DL UPT (i.e., DL-95% UPT) is increased by 10.1% ∼ 14.6%. The mean UL UPT is increased by 107.8% ∼ 246.3%, which is much higher than the UL resource increase. For cell-edge UEs, the UL UPT (i.e., UL-5% UPT) is increased by 116.2% ∼ 123.0%. For cell-center UEs, the UL UPT (i.e., UL-95% UPT) is increased by 100.2% ∼ 216.2%. The UL UPT gain in case of high RU is much higher than that for low/medium RU especially for cell-centre UEs since uplink is the bottom neck of baseline TDD in case of high traffic load.

According to the simulation results as shown in Fig. 18, different packet latency is achieved with different SBFD patterns. For SBFD pattern 1, the DL 50th percentile latency is identical to that for baseline TDD in case of low and medium RU while it is slightly increased by 7.7% in case of high RU. The UL 50th percentile latency is decreased by 61.1%, 64.7% and 80.9% for low RU, medium RU and high RU, respectively. For SBFD pattern 2, the DL 50th percentile latency is decreased by 9.1%, 13% and 15.4% for low RU, medium RU and high RU, respectively. The UL 50th percentile latency is decreased by 61.1%, 64.7% and 81.5% for low RU, medium RU and high RU, respectively.

From Fig. 19 and Fig. 20, observations on UPT for URLLC traffic and SBFD pattern 1 under dense urban

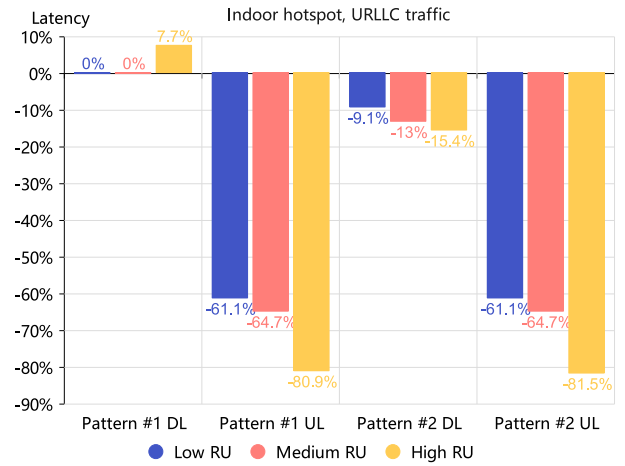

FIGURE 18. 50%-tile latency for indoor hotspot with URLLC traffic.

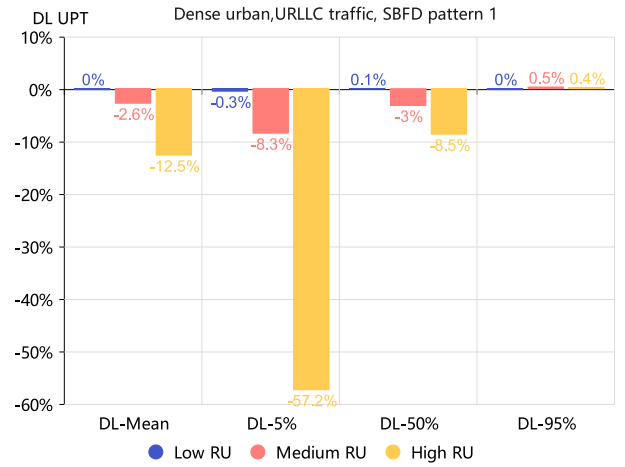

FIGURE 19. DL UPT for dense urban macro with URLLC traffic and SBFD pattern 1.

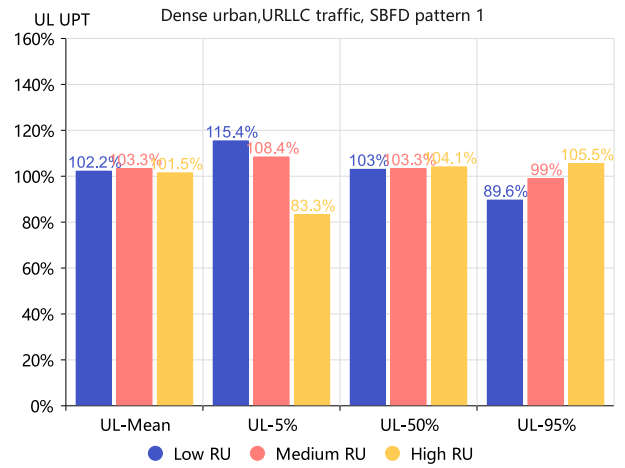

FIGURE 20. UL UPT for dense urban macro with URLLC traffic and SBFD pattern 1.

scenarios can be summarized from the DL and UL perspective separately. The DL mean UPT is basically identical to that for baseline TDD in case of low and medium RU. However, the DL mean UPT is decreased by 12.5% in case

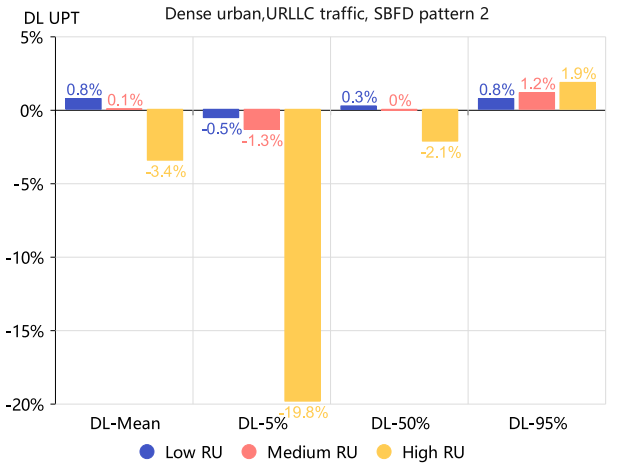

FIGURE 21. DL UPT for dense urban macro with URLLC traffic and SBFD pattern 2.

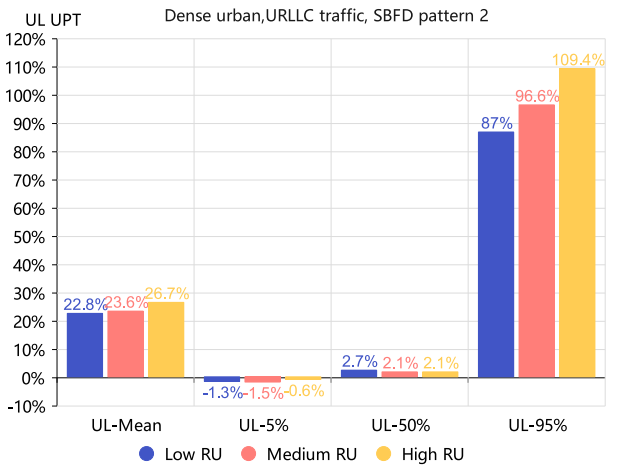

FIGURE 22. UL UPT for dense urban macro with URLLC traffic and SBFD pattern 2.

of high RU due to UE-UE CLI and reduced DL resource. For cell-edge UEs, the DL UPT (i.e., DL-5% UPT) is slightly decreased in case of low and medium RU. However, the DL UPT is decreased by 57.2% in case of high RU due to the increased UE-UE CLI. For cell-centre UEs, the DL UPT (i.e., DL-95% UPT) is the same as that for baseline TDD. In the UL, the mean UPT is increased by 101.5% $\sim$ 103.3%, which is much higher than the UL resource increase. The gain of UL UPT for cell-edge UEs and cell-centre UEs are similar, i.e., the UL UPT for cell-edge UEs and cell-centre UEs is increased by 83.3% $\sim$ 108.4% and 89.6% $\sim$ 105.5%, respectively. It is worth noting that the gain decreases with the increase of traffic load for cell-edge UEs, while the gain increases with the increase of traffic load for cell-center UEs. This implies that cell-edge UEs are more vulnerable to gNB-side interference compared with cell-center UEs.

Fig. 21 and Fig. 22 provide the results on UPT for URLLC traffic with SBFD pattern 2 under dense urban scenarios. Specifically, the DL mean UPT is basically identical to that for baseline TDD in case of low and medium RU, while it experiences 3.4% decrease in case of high RU due

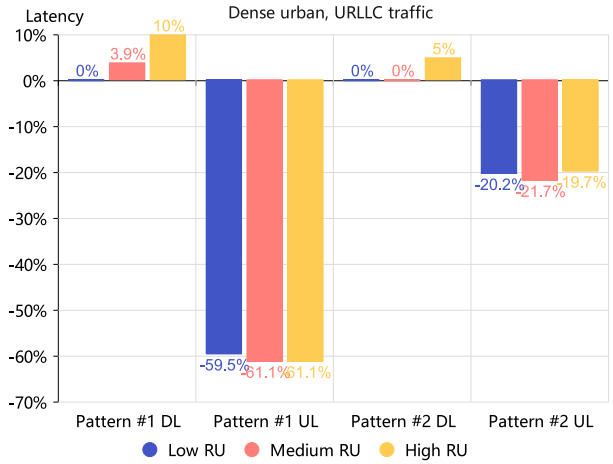

FIGURE 23. 50%-tile latency for dense urban macro with URLLC traffic.

to increased UE-UE CLI. The DL UPT for cell-edge UEs is almost the same as that for baseline TDD in case of low and medium RU, while it experiences a 19.8% decrease in case of high RU due to the UE-UE CLI. For cell-centre UEs, the DL UPT is almost the same as that for baseline TDD. For the UL, mean UPT is increased by 22.8% $\sim$ 26.7%. There is no obvious gain or loss observed for the UL UPT for cell-edge UEs, i.e., the UL-5% UPT is basically the same as that for baseline TDD. For cell-centre UEs, the UL UPT (i.e., UL-95% UPT) is increased by 87% $\sim$ 109.4%. Unlike other cases, the UPT gain is increasing with the traffic load. The reason is that, the UL UPT for baseline TDD decreases with the increasing RU due to the limited UL transmission chance in each TDD period for baseline TDD.

Fig. 23 depicts the packet latency for URLLC traffic under dense urban scenarios. For SBFD pattern 1, the DL 50th percentile latency is slightly increased by less than 3.9% for low RU and medium RU while it is increased by 10.0% in case of high RU. The UL 50th percentile latency is decreased by 59.5%, 61.1% and 61.1% for low RU, medium RU and high RU, respectively. For SBFD pattern 2, the DL 50th percentile latency is basically identical to that for baseline TDD. The UL 50th percentile latency is decreased by 20.2%, 21.7% and 19.7% for low RU, medium RU and high RU, respectively.

3) SUMMARY OF THE SIMULATION RESULTS

The performance of UPT and latency is mainly impacted by scenarios, SBFD patterns, traffic type, traffic load and location of UEs. Specifically, regarding SBFD pattern 1, two factors may impact the DL UPT, i.e., reduced DL resources and UE-UE CLI, both of which have negative impact on the DL UPT. For UL, the baseline TDD only has one transmission occasion in each TDD period, while SBFD pattern 2 has five transmission occasions. Thus, for UL UPT, the increased UL transmission opportunities have positive impact on it, while the gNB-side interference has negative impact on it.

TABLE 3. Summary of UPT gain or loss under the indoor hotspot scenario.

UPT gain/loss for indoor hotspot			Low RU		Medium RU		High RU	
			Cell-edge	Cell-centre	Cell-edge	Cell-centre	Cell-edge	Cell-centre
SBFD pattern 1	URLLC	DL	~	~	~	~	↓↓↓	~
		UL	↑↑↑↑	↑↑↑↑	↑↑↑↑	↑↑↑↑	↑↑↑↑	↑↑↑↑
	eMBB	DL	↓↓	↓↓	↓↓	↓↓	↓↓↓	↓↓
		UL	↑↑↑	↑↑↑	↑↑↑↑	↑↑↑	↑↑↑↑	↑↑↑
SBFD pattern 2	URLLC	DL	↑	↑	↑	↑	↓↓	↑
		UL	↑↑↑↑	↑↑↑↑	↑↑↑↑	↑↑↑↑	↑↑↑↑	↑↑↑↑
	eMBB	DL	~	↓	~	↓	↓↓	↓
		UL	~	↑	↑	↑	↓	↑

TABLE 4. Summary of UPT gain or loss under the dense urban macro scenario.

UPT gain/loss for dense urban macro			Low RU		Medium RU		High RU	
			Cell-edge	Cell-centre	Cell-edge	Cell-centre	Cell-edge	Cell-centre
SBFD pattern 1	URLLC	DL	~	~	↓	~	↓↓↓	~
		UL	↑↑↑↑	↑↑↑	↑↑↑↑	↑↑↑↑	↑↑↑	↑↑↑↑
	eMBB	DL	↓↓	↓	↓↓	↓	↓↓↓	↓
		UL	↑↑↑↑	↑↑↑	↑↑↑↑	↑↑↑	↑↑	↑↑↑
SBFD pattern 2	URLLC	DL	~	~	~	~	↓	~
		UL	~	↑↑↑	~	↑↑↑↑	~	↑↑↑↑
	eMBB	DL	~	~	~	↑	~	~
		UL	↑	↑	↑↑	↑↑	~	↑↑

Similarly, regarding SBFD pattern 2, the UE-UE CLI has negative impact on the DL UPT, while the increased DL transmission occasion in each TDD period has positive impact on the DL UPT. For UL, the baseline TDD only has one transmission occasion in each TDD period, while SBFD pattern 2 has five transmission occasions. Thus, for UL UPT, the increased UL transmission opportunities have positive impact on it, while the gNB-side interference has negative impact on it.

The overall simulation results of UPT for indoor hotspot and dense urban macro are summarized in Table 3 and Table 4, respectively. The symbol "$\sim$" indicates that the UPT performance gain or loss is in the range of [-5%, 5%] and essentially means little impact to the system. The upper arrow symbol "$\uparrow$" represents a positive gain in the performance with one, two, three and four symbols indicating a performance gain within the range of (5%, 20%], (20%, 50%], (50%, 90%] and larger than 90%, respectively. Similarly, the down arrow symbol "$\downarrow$" indicates a performance loss, with one, two, three and four symbols indicating a performance loss within the range of (5%, 20%], (20%, 50%], (50%, 90%] and larger than 90%, respectively.

For indoor hotspot scenario, as shown in Table 3, some observations can be made. For SBFD pattern 1 with eMBB traffic, the DL UPT experiences obvious loss for both cell-edge UE and cell-centre UE for all traffic loads. However, for SBFD pattern 1 with URLLC traffic, no obvious gain or loss is observed for DL UPT for both cell-edge UE and

cell-centre UE for all traffic loads except that obvious loss is observed for cell-edge UE in case of high traffic load. For SBFD pattern 2 with eMBB traffic, small loss of DL UPT is observed for cell-centre UEs for all traffic loads and obvious loss of DL UPT is observed for cell-edge UE in case of high traffic load. On the contrary, For SBFD pattern 2 with URLLC traffic, DL UPT experiences small gain for both cell-edge UE and cell-centre UE for all traffic loads, except that obvious loss is observed for cell-edge UE in case of high traffic load. Overall, UL UPT gain is observed in almost all cases. For SBFD pattern 1 with either eMBB traffic or URLLC traffic, significant UL UPT gain is observed for both cell-edge UE and cell-centre UE for all traffic loads. Overall, the UL UPT gain for URLLC traffic is higher than that for eMBB traffic. For SBFD pattern 2 with eMBB traffic, small gain is observed for both cell-edge UE and cell-centre UE for all traffic loads, except that small UL UPT loss is observed for cell-edge UEs in case of high traffic load. While for SBFD pattern 2 with URLLC traffic, significant gain is observed for UL UPT for both cell-edge UE and cell-centre UE for all traffic loads.

Table 4 presents the results under dense urban scenarios. For SBFD pattern 1 with eMBB traffic, the DL UPT experiences obvious loss for cell-edge UE and small loss for cell-centre UE for all traffic loads. For SBFD pattern 1 with URLLC traffic, no obvious gain or loss is observed for DL UPT for cell-centre UE for all traffic loads, while obvious DL UPT loss is observed for cell-edge UE especially for the case of high RU. For SBFD pattern 2 with eMBB traffic, no obvious gain or loss is observed for DL UPT for both cell-edge UE and cell-centre UE for all traffic loads, except that small gain is observed for cell-centre UE in case of medium traffic load. For SBFD pattern 2 with URLLC traffic, no obvious gain or loss is observed for DL UPT for both cell-edge UE and cell-centre UE for all traffic loads, except that small loss is observed for cell-edge UE in case of high traffic load.

For SBFD pattern 1 with either eMBB traffic or URLLC traffic, significant UL UPT gain is observed for both cell-edge UE and cell-centre UE for all traffic loads. For SBFD pattern 2 with eMBB traffic, small/medium gain is observed for cell-edge UE and cell-centre UE for all traffic loads. While for SBFD pattern 2 with URLLC traffic, significant gain is observed for UL UPT for cell-centre UE for all traffic loads, but no obvious gain or loss is observed for cell-edge UE. Generally speaking, UL UPT gain is observed in all cases for cell-centre UE, there is some cases without obvious gain or loss for UL UPT for cell-edge UE.

Overall, for both indoor hotspot scenarios and dense urban macro scenarios, DL UPT suffers larger loss for eMBB traffic than that for URLLC traffic since eMBB traffic is more likely to cause CLI due to its longer contiguous transmission duration. DL UPT for SBFD pattern 2 outperforms that for SBFD pattern 1 due to its increased DL transmission chances and the reduced DL resource for SBFD pattern 1. Cell-edge UEs suffer obvious DL UPT loss in case of high traffic load. On the other hand, UL UPT experiences larger gain for URLLC traffic than that for eMBB traffic especially for cell-centre UE since eMBB traffic is more likely to cause CLI due to its longer contiguous transmission duration. For URLLC traffic, similar gain is observed for UL UPT for cell-centre UE for SBFD pattern 1 and SBFD pattern 2, while UL UPT for cell-edge UE in dense urban macro scenario for SBFD pattern 1 outperforms that for SBFD pattern 2 since the UL resource in SBFD pattern 1 is increased by around 80%. Similarly, for eMBB traffic, UL UPT for SBFD pattern 1 outperforms that for SBFD pattern 2 due to the increased UL resource in SBFD pattern 1. Furthermore, the exact loss of DL UPT for cell-edge UEs is much higher than that for cell-centre UEs, especially in case of high traffic load, the loss difference between cell-edge UE and cell-centre UE is more prominent. For SBFD pattern 2 with URLLC traffic, the UL UPT gain for cell-centre UEs is much higher than that for cell-edge UEs. In general, the cell-edge UE is more vulnerable to the gNB-side interference and UE-UE CLI.

TABLE 5. Summary of latency gain or loss under the indoor hotspot and dense urban macro scenario.

Latency gain/loss			Low RU		Medium RU		High RU	
			Pattern #1	Pattern #2	Pattern #1	Pattern #2	Pattern #1	Pattern #2
Indoor hotspot	URLLC	DL	~	↑	~	↑	↓	↑
		UL	↑↑↑	↑↑↑	↑↑↑	↑↑↑	↑↑↑	↑↑↑
	eMBB	DL	↓↓	~	↓↓↓	↓	↓↓↓	↓
		UL	↑↑↑	↑	↑↑↑	↑	↑↑↑	↑↑
Dense urban macro	URLLC	DL	~	~	~	~	↓	~
		UL	↑↑↑	↑↑	↑↑↑	↑↑	↑↑↑	↑
	eMBB	DL	↓	~	↓↓	~	↓↓↓	~
		UL	↑↑↑	↑↑	↑↑↑	↑↑	↑↑	↑↑

The overall simulation results of latency for indoor hotspot and dense urban macro scenarios are summarized in Table 5. The symbol "∼" indicates that the latency performance gain or loss is in the range of [−5%, 5%] and would bring little impact to the system. The upper arrow symbol "↑" represents a positive gain in the performance with one, two and three symbols indicating a performance gain within the range of [−20%, −5%), [−40%, −20%) and larger than 40%, respectively. Similarly, the down arrow symbol "↓" indicates a performance loss, with one, two and three symbols indicating a performance loss within the range of (5%, 20%], (20%, 40%] and larger than 40%, respectively. Note that since latency is the metric being evaluated, a performance gain would mean a reduction in the latency, and vice versa.

As can be seen from Table 5, overall speaking, SBFD provides latency reduction for UL for all cases. SBFD pattern 1 outperforms SBFD pattern 2 in terms of UL latency especially for eMBB traffic in low and medium RU, because more UL resource is configured for UL in SBFD pattern 1. For DL latency, SBFD incurs negative impact for SBFD pattern1 with eMBB traffic. The DL latency is unchanged or

slightly decreased in most other cases for URLLC traffic, except that DL latency is slightly increased for SBFD pattern 1 with high URLLC traffic load due to the increased UE-UE CLI. Overall, for both DL latency, SBFD pattern 2 outperforms SBFD pattern 1 especially in case of eMBB traffic, because DL resource is reduced in SBFD pattern 1. In general, the latency performance for URLLC traffic outperforms that for eMBB traffic since eMBB traffic with larger packet size is more likely to incur interference.

C. SIMULATION RESULTS FOR COVERAGE

In order to evaluate the coverage of SBFD compared with baseline TDD, LLS plus link budget analysis is performed. Similar as the SLS, the baseline TDD applies "DDDSU" pattern and the SBFD applies SBFD pattern 1. In baseline TDD, only one UL slot is available in each TDD period, while up to 5 contiguous transmission occasions are available for SBFD pattern 1 in each TDD period. To fully explore the potential coverage of SBFD systems, the typical UL data channel in NR, the physical uplink shared channel (PUSCH), is selected as the target channel for simulation. PUSCH repetition, PUSCH repetition with joint channel estimation (JCE), PUSCH TB processing over multi-slot (TBoMS) and PUSCH TBoMS with JCE are considered in our simulation [22].

- Case 0: PUSCH is transmitted in U slot only, i.e., baseline TDD
- Case 1: Each PUSCH transmission is repeated 5 times.
- Case 2: Each PUSCH transmission is repeated 5 times with joint channel estimation, where joint channel estimation is performed over the DMRS in the SBFD slots.
- Case 3: One PUSCH TB is transmitted over 5 slots via TBoMS.
- Case 4: One PUSCH TB is transmitted over 5 slots via TBoMS together with joint channel estimation.

One of the critical issues in this LLS is to take interferences into account. In our simulation, SI, gNB-CLI and gNB-gNB CLI are considered for the PUSCH LLS. For SI, as analysed in Section II, 1 dB gNB receiver sensitivity degradation is assumed. In other words, the residual SI after all suppression methods is 6 dB under the noise floor. For gNB-CLI, the same residual interference as SI is assumed. However, the gNB-gNB CLI is difficult to have a specific value since it highly depends on the scenario, gNB transmission power, traffic load, channel model and etc. To reflect the practical gNB-gNB CLI, the average gNB-gNB CLI under different traffic loads in our SLS with urban macro scenarios is obtained. Compared with baseline TDD, the residual interference in SBFD system considering SI, gNB-CLI are gNB-gNB CLI is increased by 0.14 dB, 0.48 dB and 2.19 dB for low RU (low traffic load), medium RU (medium traffic load) and high RU (high traffic load), respectively.

The simulation assumptions for LLS are summarized in Table 6 and the required SNR for PUSCH targeting for data rate of 1 Mbps with 0.1 block error rate (BLER) obtained in our LLS simulation is summarized Table 7.

TABLE 6. Simulation assumptions for LLS.

Parameters	Value
Frequency	4 GHz
Subcarrier spacing	30 kHz
Bandwidth	100 MHz
TDD/SBFD pattern	Baseline TDD: DDDSU SFBD: XXXXU
Channel Model	TDL-C
Delay spread	300ns
UE speed	3km/h
UE Tx antenna	1
BS Rx antenna	4
Waveform	DFT-s-OFDM
PUSCH duration	14 OS
DMRS Number	2OS
Frequency hopping	disable
Number of RBs	30RBs for PUSCH repetition 5RBs for TBoMS
Transmission block size	2600 bits
Hybrid automatic repeat request	disable
Target BLER	10%

TABLE 7. Required SNR for PUSCH with 0.1 BLER.

Case	Required SNR (dB)
Case 0 : baseline TDD	-4.40
Case 1-1 : low RU	-9.81
Case 1-2 : medium RU	-9.61
Case 1-3 : high RU	-8.28
Case 2-1 : low RU	-10.66
Case 2-2 : medium RU	-10.40
Case 2-3 : high RU	-9.13
Case 3-1 : low RU	-2.86
Case 3-2 : medium RU	-2.56
Case 3-3 : high RU	-0.97
Case 4-1 : low RU	-3.81
Case 4-2 : medium RU	-3.54
Case 4-3 : high RU	-2.07

The maximum coupling loss (MCL) is one of the typical metrics for evaluating coverage. For coverage performance evaluation for SBFD, link budget template in this paper follows that in 3GPP coverage enhancement TR 38.830 [22] with necessary modifications. The required SNR in Table 7 is input into the link budget template to calculate the MCL and the results are summarized in Fig. 24.

As shown in Fig. 24, for PUSCH repetition, the coverage in SBFD system is improved by 4.91 dB, 4.71 dB and 3.38 dB for low RU, medium RU and high RU, respectively. For PUSCH repetition with JCE, the coverage in SBFD system is improved by 5.76 dB, 5.50 dB and 4.23 dB for low RU, medium RU and high RU, respectively, which is about 1 dB more than the case without JCE. For PUSCH TBoMS, the coverage in SBFD system is improved by 4.99 dB, 4.66 dB and 3.06 dB for low RU, medium RU and high

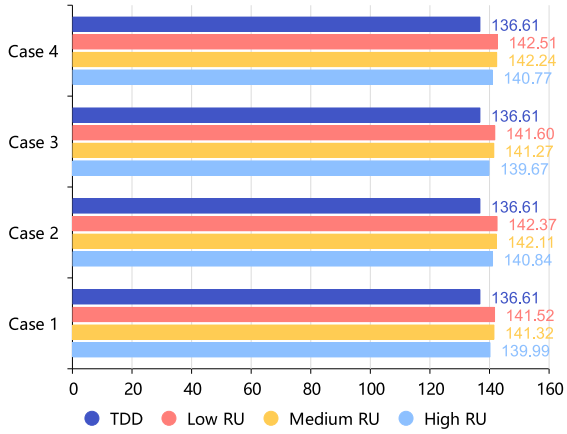

FIGURE 24. MCL results of different cases for SBFD.

TABLE 8. Configurations of the SBFD field test.

Parameter	Value
Frequency	4.9 GHz
BS antenna configuration	4T4R
UE antenna configuration	2T4R
Base station Tx power	1000 mw
SBFD pattern	DXXXU
Bandwidth	100 MHz for DL/UL slot, 10 MHz for DL subband, 90 MHz for UL subband
Antenna isolation	21.5 cm

RU, respectively, which is slightly less than that for PUSCH repetition. For PUSCH TBoMS with JCE, the coverage in SBFD system is improved by 5.90 dB, 5.63 dB and 4.16 dB for low RU, medium RU and high RU, respectively.

IV. FIELD TEST OF SBFD

In [10], a PoC on SBFD is implemented and tested in the laboratory. To further explore the practical performance of SBFD system, in this paper, an outdoor field test is carried out on the roof of a building. To explore the extreme uplink throughput performance, the SBFD gNB applies DXXXU pattern, where around 10 MHz and 90 MHz are allocated for DL subband and UL subband in the "X" slot, respectively. More detailed configurations are described in Table 8.

During the tests, two types of commercial 5G UEs are involved, namely, the ZTE Axon 20 and ZTE Axon 30. In the field tests, the antenna height of the BS and the UE is around 1 m and 0.5 m, respectively. The distance between the BS and the UE is around 1 m and thus, the propagation condition between the BS and UE is expected to be mostly line-of-sight (LOS), while there is a wall near the BS that causes reflections. Overall, the commercial UE experiences a peak uplink throughput 672 Mbps and E2E latency is around 5.3 ms.

V. DEPLOYMENT RECOMMENDATIONS FOR SBFD

According to the results obtained from both simulations and field tests, the following deployment recommendations can

FIGURE 25. Test setup for the field test of the SBFD PoC.

be madeto facilitate early deployment of SBFD in 5G-A and 6G networks.

- Both small-range cells (e.g., indoor hotpot) and medium-range cells (e.g., dense urban macro) are potential target deployment scenarios for SBFD. SBFD shows UL latency gain and UL UPT gain for almost all cases for both indoor hotspot and dense urban macro for both SBFD patterns for both cell-edge UEs and cell-center UEs. The filed test also verifies the potential deployment of SBFD for small-range cell.
- Both URLLC and eMBB are potential target services for SBFD. eMBB traffic experiences DL performance loss for both SBFD patterns for both cell-edge UEs and cell-center UEs. The DL performance loss for eMBB traffic for cell-edge UEs is larger than that for cell-centre UEs especially in case of high traffic load. Despite of the DL performance loss for eMBB traffic, the UL performance gain is much higher than the DL performance loss. For DL-centric eMBB traffic, it is better to adopt SBFD pattern 2 since the performance loss is smaller compared with SBFD pattern 1. In addition, the interference issue for cell-edge UEs should be carefully handled in this case, otherwise it will cause obvious DL performance loss.
- Both SBFD pattern 1 and SBFD pattern 2 are potential target SBFD patterns. SBFD pattern 1 has one 'UL' slot to protect the sensitive UL transmission, while SBFD pattern 2 has more DL transmission chances in each TDD period. Compared with SBFD pattern 2, the DL resource and UL resource of SBFD pattern 1 is reduced

by about 22% and increased by about 79%, respectively. SBFD pattern 1 outperforms SBFD pattern 2 in terms of UL performance and SBFD pattern 2 outperforms SBFD pattern 1 in terms of DL performance especially for eMBB traffic. This also highlights the importance of setting a proper DL/UL resource ratio for the SBFD system.

- The interference has great impact on the achievable performance gain for SBFD. Advanced CLI handling schemes should be studied and implemented to harvest the gain of SBFD especially for the case of high traffic load. Otherwise, the serve CLI in SBFD may even cause performance loss.
- For URLLC traffic that is sensitive to UL latency, both SBFD pattern 1 and SBFD pattern 2 can be adopted. While for URLLC traffic that is sensitive to both UL latency and DL latency, SBFD pattern 2 is more appropriate. The field test also shows SBFD's potential for E2E latency reduction.
- Coverage-limited scenarios are potential target scenarios for SBFD deployment. SBFD together with other techniques (e.g., repetition, JCE and TBoMS) provides around 3 $\sim$ 6 dB coverage gain for different cases.

VI. CONCLUSION

To explore the performance of SBFD and facilitate early deployment of SBFD in 5G-A and 6G networks, comprehensive performance evaluations on UPT, latency and coverage under different scenarios, different SBFD patterns and different traffics are conducted. Comparisons among these metrics under different scenarios, SBFD patterns and traffics are also provided and analyzed. According to the evaluation results, significant performance gains for UL UPT and UL latency are observed in SBFD systems for both cell-edge UEs and cell-center UEs across different scenarios, different SBFD patterns, different traffic types and different traffic loads. Although performance loss for DL UPT and DL latency are observed for SBFD in terms of eMBB traffic under different loads and for URLLC traffic under high loads, there is no obvious loss or even small gain for DL UPT and DL latency for SBFD with low or medium URLLC traffic load. Overall, the DL performance for SBFD pattern 2 outperforms pattern 1. Furthermore, around 3 dB $\sim$ 6 dB coverage gain is observed in SBFD systems thanks to more consecutive UL transmission instances in each TDD period.

Upon the numerical results obtained from simulations, a field test is carried out to verify the practical performance of SBFD in a typical outdoor scenario. The commercial 5G UE connecting to the SBFD base station presents 672 Mbps peak UL throughput and 5.3 ms E2E latency in outdoor scenario. In the end, some deployment recommendations for SBFD are elaborated based on the performance evaluations and field test results.

REFERENCES

[1] S. Chen, S. Sun, Y. Wang, G. Xiao, and R. Tamrakar, "A comprehensive survey of TDD-based mobile communication systems from TD-SCDMA 3G to TD-LTE(a) 4G and 5G directions," *China Commun.*, vol. 12, no. 2, pp. 40–60, Feb. 2015.

[2] A. Łukowa and V. Venkatasubramanian, "Centralized UL/DL resource allocation for flexible TDD systems with interference cancellation," *IEEE Trans. Veh. Technol.*, vol. 68, no. 3, pp. 2443–2458, Mar. 2019.

[3] X. Han, K. Xiao, R. Liu, X. Liu, G. C. Alexandropoulos, and S. Jin, "Dynamic resource allocation schemes for eMBB and URLLC services in 5G wireless networks," *Intell. Converged Netw.*, vol. 3, no. 2, pp. 145–160, Jun. 2022.

[4] X. Han et al., "Flexible spectrum orchestration of carrier aggregation for 5G-advanced," May 2023, *arXiv:2305.15890*.

[5] R. Liu, H. Lin, H. Lee, F. Chaves, H. Lim, and J. Sköld, "Beginning of the journey towards 6G: Vision and framework," *IEEE Commun. Mag.*, submitted for publication.

[6] C.-X. Wang et al., "On the road to 6G: Visions, requirements, key technologies, and testbeds," *IEEE Commun. Surveys Tuts.*, vol. 25, no. 2, pp. 905–974, 2nd Quart., 2023.

[7] W. Chen et al., "5G-advanced toward 6G: Past, present, and future," *IEEE J. Sel. Areas Commun.*, vol. 41, no. 6, pp. 1592–1619, Jun. 2023.

[8] R. Liu et al., "6G enabled advanced transportation systems," May 2023, *arXiv:2305.15184*.

[9] B. Smida, A. Sabharwal, G. Fodor, G. C. Alexandropoulos, H. A. Suraweera, and C.-B. Chae, "Full-duplex wireless for 6G: Progress brings new opportunities and challenges," *IEEE J. Sel. Areas Commun.*, vol. 41, no. 9, pp. 2729–2750, Sep. 2023.

[10] X. Han et al., "Interference mitigation for non-overlapping sub-band full duplex for 5G-advanced wireless networks," *IEEE Access*, vol. 10, pp. 134512–134524, 2022.

[11] Z. Zhang, K. Long, A. V. Vasilakos, and L. Hanzo, "Full-duplex wireless communications: Challenges, solutions, and future research directions," *Proc. IEEE*, vol. 104, no. 7, pp. 1369–1409, Jul. 2016.

[12] D. Kim, H. Lee, and D. Hong, "A survey of in-band full-duplex transmission: From the perspective of PHY and MAC layers," *IEEE Commun. Surveys Tuts.*, vol. 17, no. 4, pp. 2017–2046, 4th Quart., 2015.

[13] X. Lin, "An overview of 5G advanced evolution in 3GPP release 18," *IEEE Commun. Stand. Mag.*, vol. 6, no. 3, pp. 77–83, Sep. 2022.

[14] M. Mokhtari, G. Pocovi, R. Maldonado, and K. I. Pedersen, "Modeling and system-level performance evaluation of sub-band full duplexing for 5G-advanced," *IEEE Access*, vol. 11, pp. 71503–71516, 2023.

[15] "Study on evolution of NR duplex operation," 3GPP, Sophia Antipolis, France, Rep. TR 38.858, 2022. [Online]. Available: https://portal.3gpp.org/desktopmodules/Specifications/SpecificationDetails.aspx?specificationId=3984

[16] H. Ji et al., "Extending 5G TDD coverage with XDD: Cross division duplex," *IEEE Access*, vol. 9, pp. 51380–51392, 2021.

[17] "NR; user equipment (UE) radio transmission and reception; part 1: Range 1 standalone," 3GPP, Sophia Antipolis, France, Rep. TR 38.101-1, 2018. [Online]. Available: https://portal.3gpp.org/desktopmodules/Specifications/SpecificationDetails.aspx?specificationId=3283

[18] M. Z. Chowdhury, M. Shahjalal, S. Ahmed, and Y. M. Jang, "6G wireless communication systems: Applications, requirements, technologies, challenges, and research directions," *IEEE Open J. Commun. Soc.*, vol. 1, pp. 957–975, 2020.

[19] L. Tian, S. Wang, Z. Cheng, and X. Bu, "All-digital self-interference cancellation in zero-IF full-duplex transceivers," *China Commun.*, vol. 13, no. 11, pp. 27–34, Nov. 2016.

[20] "Study on new radio access technology: Physical layer aspects," 3GPP, Sophia Antipolis, France, Rep. TR 38.811, 2019. [Online]. Available: https://portal.3gpp.org/desktopmodules/Specifications/SpecificationDetails.aspx?specificationId=3066

[21] R. Liu, R. Yu-Ngok Li, M. Di Renzo, and L. Hanzo, "A vision and an evolutionary framework for 6G: Scenarios, capabilities and enablers," May 2023, *arXiv:2305.13887*.

[22] "NR coverage enhancements," 3GPP, Sophia Antipolis, France, Rep. TR 38.830, 2020. [Online]. Available: https://portal.3gpp.org/desktopmodules/Specifications/SpecificationDetails.aspx?specificationId=3734

XINGGUANG WEI received the M.S. degree from the Beijing University of Posts and Telecommunications, China, in 2018. Since 2018, he has been working with ZTE Corporation as a Standardization Engineer. He has been involved in 3GPP 5G standardization since the first NR release, i.e., Rel-15, mainly focusing on bandwidth part, carrier aggregation, ulticast/broadcast, and full duplex.

JIAN LI received the M.S. degree from the Chongqing University of Posts and Telecommunications, China, in 2010. Since 2010, he has been working with ZTE Corporation as a Research Engineer. His research interests include interference coordination, carrier aggregation, bandwidth part, coverage enhancement, and full duplex.

CHUNLI LIANG received the M.S. degree from Xiamen University, China, in 2005. She has been working with ZTE Corporation as a Research Engineer since 2006. Her research interests include synchronization signal design, physical uplink channel design, carrier aggregation, full duplex, enhancement of ultrareliable and low-latency, coverage enhancement, and multicarrier operations.

XIANGHUI HAN received the M.S. degree in communication and information system with the Beijing University of Posts and Telecommunications in 2015. He is currently pursuing the D.Eng. degree in electronic information from Southeast University. Since 2015, he has been working with ZTE Corporation as a Standard Engineer. He actively participates in standardization work in 3GPP RAN1 Working Group, involving in 5G topics, such as ultrareliable and low-latency communications, coverage enhancement, sub-band full duplex operations, and dynamic spectrum sharing. He is the RAN1 Feature Lead of several enhancements in Rel-17 and Rel-18.

MIN REN received the M.S. degree from Xidian University, China, in 2010. Since 2010, she has been working with ZTE Corporation as a Simulation Engineer. She has been involved in the 3GPP 5G standardization since the first NR release, i.e., Rel-15, mainly focusing on ultra-reliable low-latency, carrier aggregation, coverage enhancement, and full duplex.

RUIQI (RICHIE) LIU (Member, IEEE) received the B.S. and M.S. degrees (with Hons.) in electronic engineering from the Department of Electronic Engineering, Tsinghua University in 2016 and 2019, respectively. He is currently a Master Researcher with the Wireless and Computing Research Institute, ZTE Corporation, responsible for long-term research as well as standardization. He is the author or coauthor of several books and book chapters. He has participated in national key research projects as a researcher or a research lead. During his three-year service at 3GPP from 2019 to 2022, he has authored and submitted more than 500 technical documents with over 100 of them approved, and he served as the co-rapporteur of the work item on NR RRM enhancement and the feature lead of multiple features. His main research interests include reconfigurable intelligent surfaces, integrated sensing and communication, and wireless positioning. His recent awards include the 2022 SPCC-TC Outstanding Service Award and the Beijing Science and Technology Invention Award (Second Prize) in 2022. He currently serves as the Vice Chair of ISG RIS in the ETSI. He actively participates in organizing committees, technical sessions, tutorials, workshops, symposia, and industry panels in IEEE conferences as the chair, an organizer, a moderator, a panelist, or an invited speaker. He served as the Guest Editor for *Digital Signal Processing* and a Lead Guest Editor for the special issue on 6G in IEEE OPEN JOURNAL OF THE COMMUNICATIONS SOCIETY. He serves as the Deputy Editor-in-Chief for *IET Quantum Communication* and an Editor for *ITU Journal of Future and Evolving Technologies*. He is the Standardization Officer of IEEE ComSoc ETI on reconfigurable intelligent surfaces and the Standards Liaison Officer of IEEE ComSoc Signal Processing and Computing for Communications Technical Committee.